L Berkeley National L y	Cat Code	ENGINEERING Note	Serial #	Rev **A**	Page 1 of 30
Author(s) Heng Pan, S. Prestemon	Department Mechanical Engineering	Location Berkeley	Date 6/16/2011		
Title MICE Spectrometer Solenoid Magnet Protection Analysis					

Executive summary

The spectrometer solenoid quench protection system is analyzed to fully understand the quench initiation and propagation process under various conditions, and to determine what modifications should be made to fully protect the system under fault conditions. In particular, detailed 3D simulations are provided to quantify the current transients during quench events, and to evaluate quench propagation via quenchback due to eddy-current generation in the Aluminum mandrel.
The analysis indicates that:

1) Quenchback will occur, although the timescale for full system de-energization depends on quench initiation point and operating current at quench onset.
2) Quench hot-spot temperatures are typically below ~120K, although values of ~130 can be generated under some conditions. These values are typical of superconducting magnet systems.
3) Peak internal turn-to-turn voltages are negligible, and layer-to-layer voltages do not exceed ~200V. These values are acceptable based on the coil design and fabrication.
4) Voltage to ground can become significant, reaching as high as ~1600V at peak operating current. The coils have been tested to 5kV during assembly. the calculations indicate that the voltages are acceptable.

The simulations of various coil quench configurations indicate that the existing passive protection system will adequately protect the magnet under "routine" quench scenarios. This is consistent with the fact that a number of training quenches were generated in the magnet during previous testing campaigns, with no noticeable issue with the passive magnet protection circuitry.
Under more serious fault conditions, such as an HTS or cold lead failure, the passive protection system will result in a closed-loop current decay within the magnet system, through the cold diodes and bypass resistors of the protection circuitry. Such events have occurred, with an HTS lead failure on one occasion and a burn-out of a cold LTS lead on another occasion. Under such conditions significant current is passed through the protection resistors, with long time constants. To address possible overheating of the bypass resistors, a modification to the existing design is proposed, wherein a direct conduction link is made between the existing bypass resistors and the cold-mass

structure. In the case of a lead failure the link will slow the temperature rise of the resistors, while shortening the time to quench onset. Under all fault conditions the system will lead to a safe quench de-energization without overheating the resistors.

One final modification that will be implemented is an external circuitry consisting of a switch and resistor across the power supply leads, with resistance of ~0.2 Ohms. In the case of voltage rise across the HTS leads indicating the initiation of a lead quench, the control system will open the switch and shut off the power supply. The resulting voltage rise will trigger the internal diodes, resulting in a parallel current path with the vast majority of the current flowing through the bypass resistors, thereby protecting the HTS leads.

With these modification the system is expected to perform safely under normal operating conditions and under normal quench events, and to survive serious lead fault conditions without damage to the cold-mass.

1. Introduction

1.1. Background

The MICE spectrometer solenoids modifications are in progress now at the vendor's site. The previous test and analysis showed a high risk that overheating may occur in the bypass resistors under certain quench or fault conditions. For the solenoid itself, there are two considerations that are critical for proper quench protection. First, the hot spot temperature must be kept sufficiently low, preferably below 150K. Excessive hot spot temperature can lead to large thermal stresses that can affect insulation and even the conductor. The second issue is internal voltage during the quench process. Over voltage can cause electric breakdown of insulation and possibly lead to arcing.

The quench process is therefore thoroughly analyzed to understand performance characteristics under a broad array of quench conditions, with particular attention to the role of quench-back effect. In order to analysis the passive quench protection system, and in accordance with project review recommendations, we performed various quench scenarios to quantify the adequacy of the overall protection system through the use of a 3D model and the QUENCH module by Vector Fields OPERA 3D software.

All the simulations include 3D transient magnetic field analysis (ELEKTRA) coupled with 3D thermal analysis (TEMPO) code. At each time step initially calculated transient magnetic field with corresponding induced eddy currents in the mandrel, and then shifted to thermal model to calculate the Joule heat and transient temperature in each component of model. The "quench-back" effect was taken into account in simulations by the eddy current and heat transfer calculation in mandrel.

The report focuses on worst-case scenarios, and the goal is to determine if the passive quench protection system can provide reliable protection under all scenarios that can occur during operation.

1.2. Model Introduction

The spectrometer solenoid consists of five superconducting coils (As shown in Fig.2-1): matching coils M1, M2, end coils E1, E2, and the central coil C. All coils, using Nb-Ti superconductor with a copper to superconductor ratio of 3.9, were wound on a 6061-T6 aluminum mandrel. The copper in the conductor has a minimum residual resistance ratio RRR of 70, and has insulated dimensions of 1.65 mm by 1.00 mm, (The bare dimension are 1.60 mm by 0.95 mm). The center coil is separated equally into two coils in radial direction.

The structure parameters of the magnets are listed in table 1-1.

Table 1-1 Parameters of the Spectrometer Solenoid

	M1	M2	E1	Center coil	E2
Turns/layer	120	119	66	784	66
Layers	42	28	56	20	62
Inner radius (m)	0.258	0.258	0.258	0.258	0.258
Radial thickness (m)	0.045	0.03	0.0596	0.0213	0.0660
Axial length (m)	0.201	0.199	0.111	1.314	0.111
Inner radius of mandrel (m)	0.245	0.245	0.245	0.245	0.245

A 3D model was created, which consists of all the five coils, mandrel and air region. The Spectrometer cryogenic material properties were presented by table files for proper modeling non-linear behavior in a range of 4 K -300 K (for details, see Appendix I).

Figure 1-1 3D Model of Spectrometer Solenoid

In the last series of actual coil tests, all coils (M1-M2-E1-C1-C2-E2) were connected in series and powered from a single 300 A current main power supply. Under normal operating conditions, as well as future commissioning modes, the system will be powered from three main 300A power supplies. Each match coil will be powered by a power supply that delivers 300 A; The E1-C-E2 are connected in series using a single 300 A power supply that delivers a voltage up to 10 V. In addition, the end coils E1 and E2 will be adjusted using a pair of trimming power supply that will deliver 60 A at 5 V. The external circuit of each coil has a low-resistance bypass resistor in series with back-to-back cold diodes. Fig 1-2 is the electrical scheme for simulation. Each bypass resistor has the resistance of 0.02 Ω, and external resistance is 0.2 Ω. Each diode has 4V forward voltage.

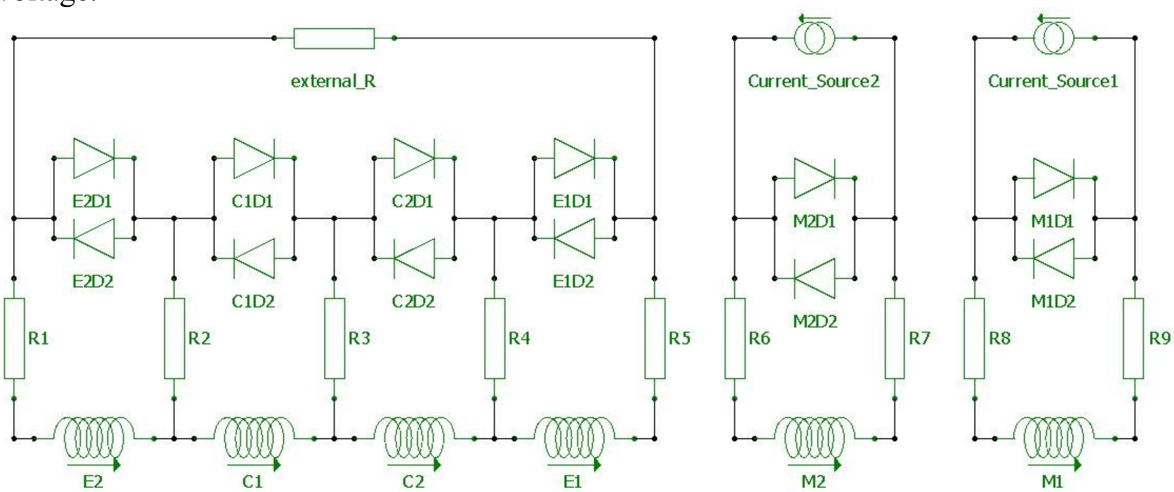

Figure 1-2 electrical scheme for simulation

The model used a time step of 0.01s, and applied different levels of mesh refinement for different component. The coil, mandrel and air near them have finer mesh, the air far away the cold mass has lower level of mesh refinement. Analysis of mesh and time step resolution is provided in appendix II.

2. Quench scenarios

The central coil has the largest stored energy among the solenoids. Furthermore, the center coil has a length of 1.314 meters, which is about 6~13 times longer than other coils; it has a high probability that a quench will take place in some parts of it under normal operation. So, quench starts in central coil is a typical case in normal operation.

On the other hand, the central coil is long compared to its thickness. A quench starting at one end will take a long time to propagate to the other end. And the time for the central coil become fully normal is the longest among all the five coils. From a quench standpoint, it is the worst case for the central coil that a quench starts from one end.

The other aspect is that a quench in one coil will heat the neighboring coil with a relatively delay time by quench-back effect. It is expected that all the five coils can come to fully normal as soon as possible when a quench happens in one of them. But obviously, the time delay of quenches may put some parts of leads in danger. M1 coil is the farthest one from the central coil, and quench starts from M1 coil will take the longest time to propagate to E2 coil.

Therefore, it is the worst case if quench starts from M1 coil. Peak hot-spot and voltage values are not necessarily obtained from quenches at maximum operating current; therefore four scenarios were performed:

N1: the initial quench position is on the middle of the inner surface of the center coil; the initial current is 265A.

N2: the M1 coil is triggered quench initially. The initial current is 265A.

N3: the M1 coil is triggered quench initially. The initial current is 200A.

N4: the M1 coil is triggered quench initially. The initial current is 150A.

The power supplies for match coils are remained in the circuit to maintain a constant current output. The initial heat will be injected to coil by a circle film heater.

3. Hot-spot and internal voltage results

3.1 Scenario 1

The initial current is 265A; a quench was initiated in the C1 coil. As showed in figure 3-1, all currents dropped to 15A after 10s. The M1 coil, which is far away from the quenched C1 coil, was triggered to quench in 3s. The C1 and C2 coils took about 4s from quench-initiation to the peak temperature of 100K. All the other coils ultimately reached a peak temperature of about 80K. The bypass resistors of E1 and E2 carried a current from 265A to 0 A during 10s.

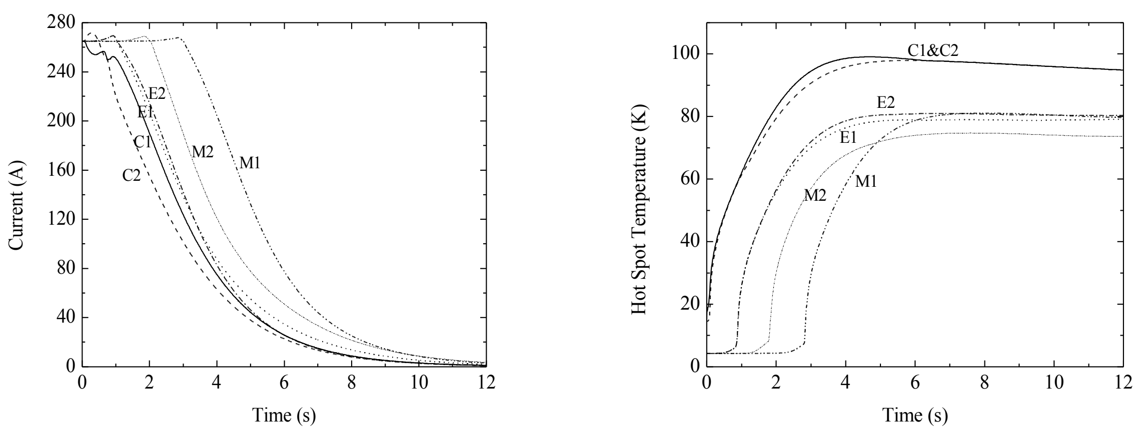

Figure 3-1 current decay (left) and hot spot temperature (right) of all coils

3.2 Scenario 2

The initial current is 265A; but a quench was initiated in the M1 coil. Figure 3-2 shows the current decay and hot spot temperatures in coils. All currents dropped to 15A after 11s, which is a little longer than that in scenario 1. It is the worst case in that it took the longest time to make all coils quench. The E2 coil, which is far away from the quenched M1 coil, was triggered to quench in 4s. Because the normal zone in the central coil has to propagate from one end to the other, which means the propagation will take longer time, the hot spot temperature reached the peak value of 116 K. For other coils, the peak temperature is around 80K. The bypass resistors of E1 and E2 carried a current from 265A to 0 A during 12s. Significantly, in the first 4s the current in the bypass resistor of E1 remained near a constant value of 265A.

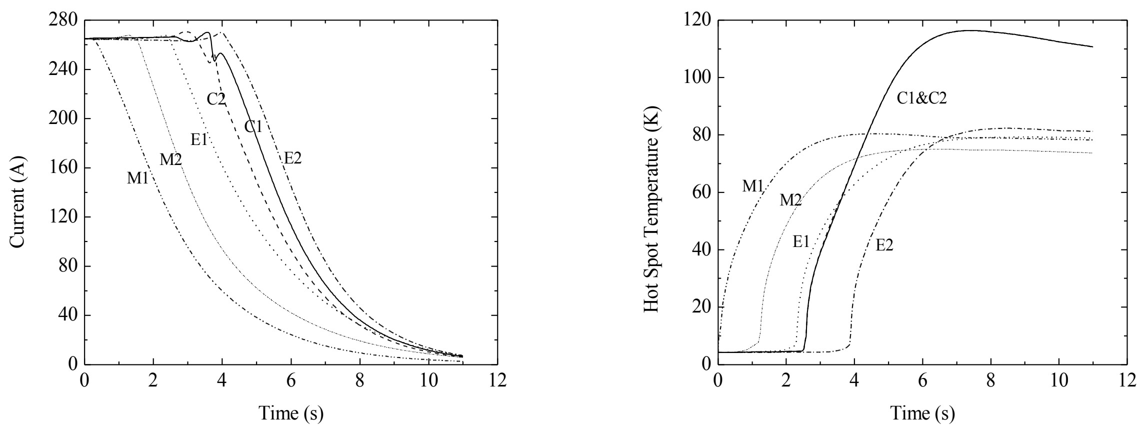

Figure 3-2 current decay (left) and hot spot temperature (right) of all coils

3.3 Scenario 3

The initial current is 200A; a quench was initiated in the M1 coil. All currents dropped to 15A after 16s. The propagation time alone the whole solenoids became longer. Compared to the scenario 2, the hot spot temperature in this scenario is lower though the propagation took a longer time. The peak temperature is 81K in C2 coil. The hot spot temperature in other coils dropped to around 60K. Results are shown in Figure 3-3.

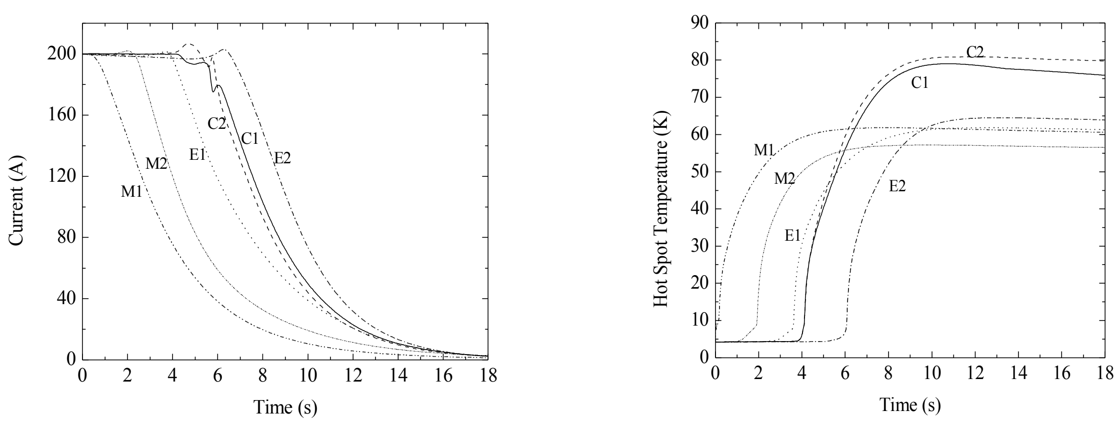

Figure 3-3 current decay (left) and hot spot temperature (right) of all coils

3.4 Scenario 4

The initial current is 150A; a quench was initiated in the M1 coil. All currents dropped to 15A after 19s. The propagation time alone the whole solenoids became further longer.

One could see that the lower quench current, the longer quench propagation along the solenoid, and the longer current decay in the far away coils from the quenched one. Compared to the previous scenarios, the peak temperature in this case dropped to 60K, which is in C2 coil. The hot spot temperature in other coils dropped to around 50K. Results are shown in Figure 3-4.

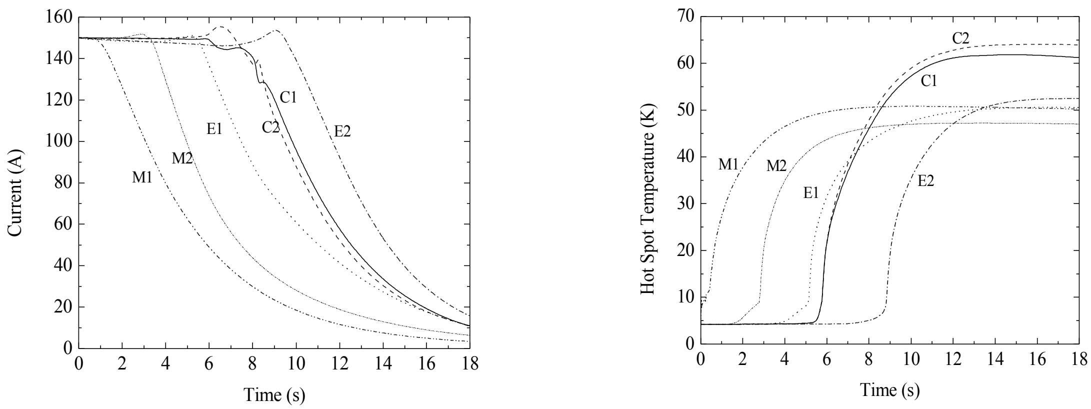

Figure 3-4 current decay (left) and hot spot temperature (right) of all coils

Therefore, high operation current results in higher hot-spot temperature, though lower current induces longer propagation time. The hot spot temperature in the worst case is 116K. This is acceptable for adiabatic solenoids and indicates that typical quench scenarios are well-protected.

3.5 Internal voltage

The other issue during quench is internal voltage. Internal voltage main includes interlayer voltage and peak ground voltage. To calculate these terms, a coil is treated as turn elements connected in series, and each turn element is a combination of resistance and inductance. Then the resultant voltage is the sum of these two opposite components:

$$V_i = V_{i-1} + \sum_{j=1}^{N} L_{i,j} \frac{dI}{dt} + R_i I_i \qquad (4\text{-}1)$$

In the expression, $V_{i\text{-}1}$ is the voltage of turns i-1; $L_{i,j}$ is the mutual inductance of turn i and j. I is the transient current; R_i is the resistance of turn i:

$$R_i(T) = \rho_i(T)\frac{l_i}{S_i} \qquad (4\text{-}2)$$

S_i is the cross area of copper component of wire, ρ_i is the resisticity of copper; The mutual inductance can be obtained by the following:

$$L_{ij} = \mu_0\sqrt{R_i R_j}\left[\left(\frac{2}{k} - k\right)K(k) - \frac{2}{k}E(k)\right] \qquad (4\text{-}3)$$

Where, the elliptic functions are:

$$K(k)=\int_0^{\pi/2}\frac{d\phi}{\sqrt{1-k^2\sin^2\phi}} \quad (4\text{-}4)$$

$$E(k)=\int_0^{\pi/2}\sqrt{1-k^2\sin^2\phi}\,d\phi \quad (4\text{-}5)$$

$$k=\sqrt{\frac{4R_iR_j}{\left(R_i+R_j\right)^2+z^2}} \quad (4\text{-}6)$$

R_i and R_j are the average radius of turns i and j. The peak voltage to ground in the coil V_{max} is float; we need to find the maximum local voltage and minimum local voltage within the coil. The difference is the peak voltage to ground of the coil.

$$V_{\max}=\left|\max\{V_i|i=1,2,\cdots,N_{\text{coil}}\}-\min\{V_i|i=1,2,\cdots,N_{\text{coil}}\}\right| \quad (4\text{-}7)$$

Where, N_{coil} is the sections number. For the insulations, the interlayer voltage is corresponding to layer-to-layer insulation; and peak ground voltage is corresponding to G-10 sheet between coil and mandrel.

Internal voltage is mainly affected by local temperature and current-transients. The central coil definitely has the maximum temperature, so we focused on the central coil. The figure 3-5 shows the maximum interlayer voltage and peak ground voltage at 265A. The maximum interlayer voltage is 200V, and the peak ground voltage is 1600V, compared the value of 3000V without subdivision protection.

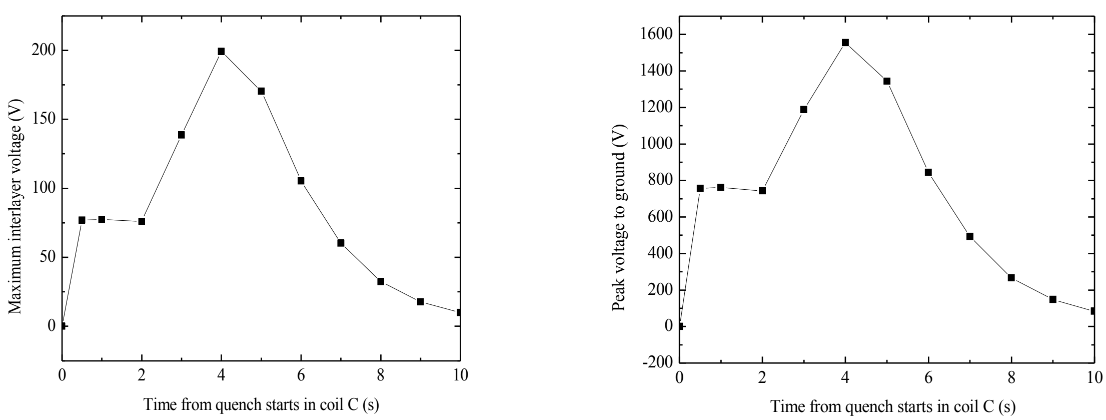

Figure 3-5 Interlayer voltage and peak ground voltage (265A)

When the current is 200A, the two kinds of internal voltage dropped a lot. The maximum interlayer voltage dropped to 90V, and peak ground voltage dropped to 800V (Fig. 4-6).

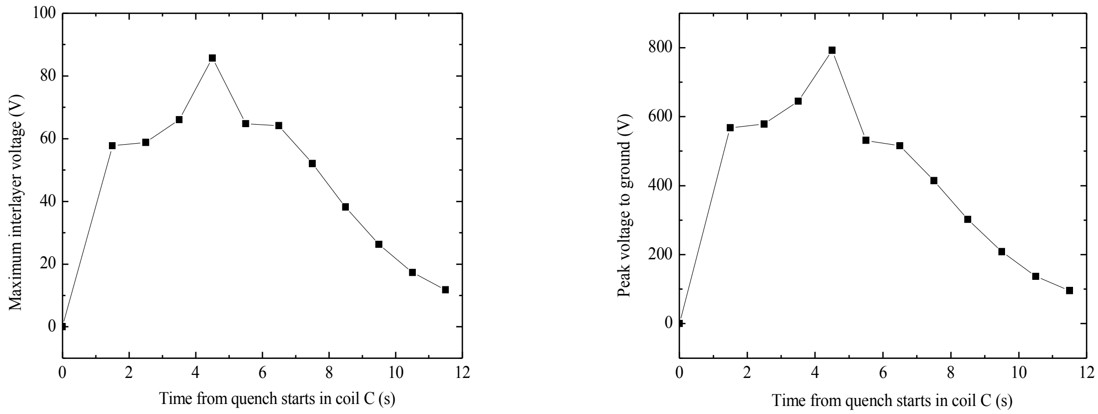

Figure 4-6 Interlayer voltage and peak ground voltage (200A)

When the current reduced to 150A, the two voltages dropped to 50V and 460V (Fig. 4-7).

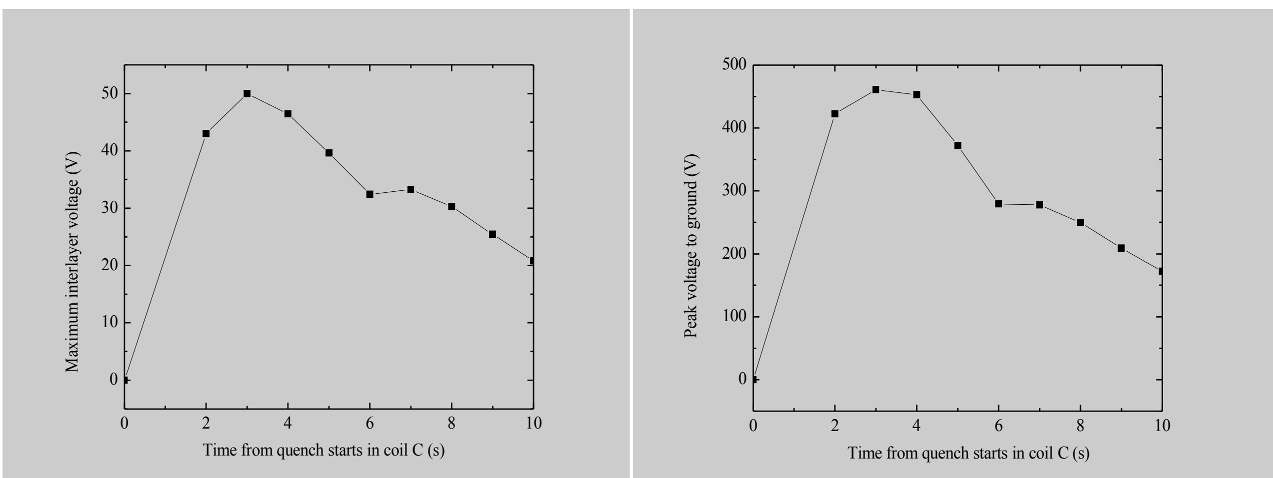

Figure 4-7 Interlayer voltage and peak ground voltage (150A)

In fact, the peak ground voltage is floating potential. For a coil with subdivision, the terminal voltage of each section is very small (near the forward voltage of diodes), the peak ground voltage of the whole coil is approximated by the peak ground voltage of each section. Therefore, subdivision protection can reduce almost half peak ground voltage.

4. Passive protection system

The original magnet protection system was designed using cold diodes in series with bypass resistors across each of the individual magnets, and, in the case of the central solenoid, across the two (radially separated) coils that form the solenoid (see figure 4-1). This "passive" protection scheme is standard practice in large commercial multi-coil magnet systems, as it decouples magnets during a quench, allowing for faster current decay, lower internal voltages, and lower hot-spot temperatures, but does not require an active detection and heater circuit that would add complexity and additional failure modes to the system. Here we propose two modifications to improve the protection system reliability for fault scenarios such as lead failures.

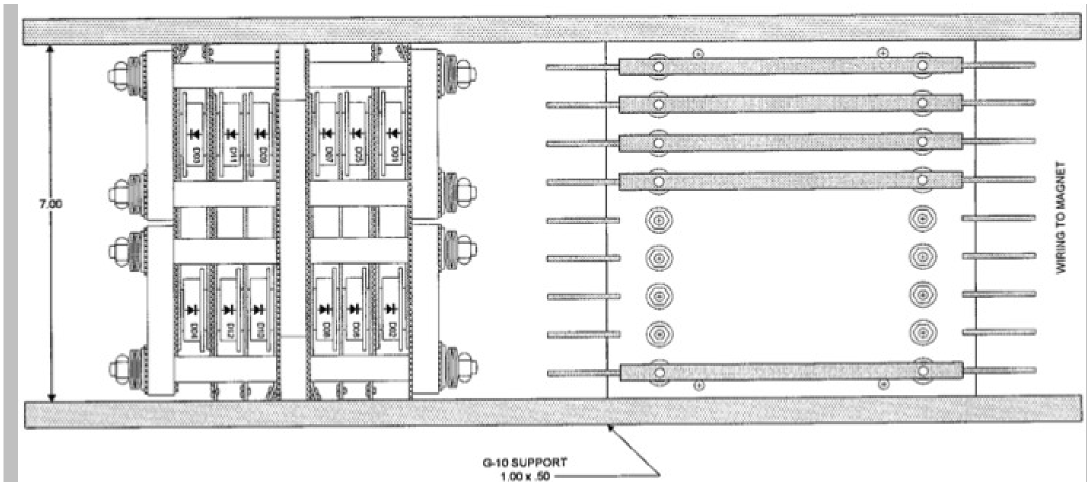

Figure 4- Basic layout of the passive protection scheme, showing the diode packs (left) and bypass resistors (right).

4.1. Bypass resistor cooling

After many training quenches of one of the MICE magnet systems, a failure of a lead occurred, which required that the cold mass be re-opened for system repair. Upon inspection of the bypass resistors, it was noted that the stainless steel resistors were discolored, and that G10 in the vicinity of the resistors had been burned. A detailed analysis of the bypass resistors under "normal" quench scenario's, e.g. those presented earlier in this report, demonstrates that the bypass resistors see acceptable, e.g. ~200K, temperature rise during a quench due to film boiling to helium (see figure 4-2). If helium is expulsed and only radiative heat transfer is assumed in the calculations, very high temperatures, ~1400K, will be reached.

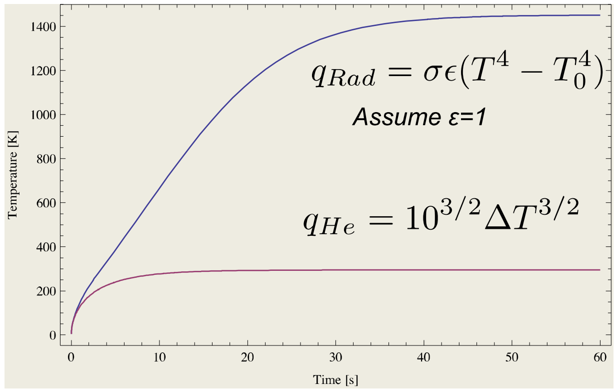

Figure 4- Temperature rise in a bypass resistor subjected to a constant 265A current, assuming a) radiative heat transfer only (q_{rad}) and film boiling to LHe only (q_{He}). Under normal quench conditions the current decay is sufficiently fast that the q_{He} regime is valid.

The fault scenarios likely to lead to high temperatures of the bypass resistors include:

1) A low-current quench, resulting in extended decay times and slow quenchback to other coils;
2) Failure of leads (e.g. HTS leads), resulting in a closed-loop current path in the cold mass through the bypass resistors and a slow decay of the current.

In both cases the passive protection system must be designed to support the current through the bypass resistors until the system quenches and the stored energy is deposited in the coils. Although the system as initially designed had survived many quenches, as well as a lead failure, the resistor discoloration suggested that very high temperatures had existed in the resistors. Two approaches to mitigating the resistor overheating have been evaluated:

a) Thermally link the bypass heaters to the cold mass so as to moderate the resistor temperature rise and reliably generate propagating coil quenches when bypass current exists;
b) The introduction of active heaters to force a quench in a coil once current is detected in the bypass resistors.

Option (b) has the advantage of allowing for induced quenches during training and/or during operation. However, active systems are best designed into the initial system. The introduction of an active circuit into an existing system adds significant risk as well as additional diagnostic and control complexity.

Here we have decided to pursue option (a) based on the following observations:

1. The system has quenched safely through many training quenches;
2. The system has survived serious fault conditions without serious damage to the cold mass, and
3. The simulations clearly indicate that quenchback reliably propagates quenches from one coil to the next, and with

reasonable time constants resulting in acceptable hot-spot temperatures and internal voltages.

To implement option (a), a modification to the system is proposed, wherein the bypass resistors are thermally connected to nearby members of the cold mass structure, this will slow the temperature rise of the resistors while hastening the onset of coil quenches.

The conceptual design of the thermal link is shown in Figure 4-4. The stainless steel bypass resistors are insulated with ceramic fiber sleeves that provide robust electrical insulation. The insulated resistors are then clamped between Copper plates; the upper Copper plate is bolted to existing Aluminum rails located in the cold mass. The modifications will allow for ample cooling of the bypass resistors under all quench and fault scenarios.

To validate the approach, an experiment has been developed and measurements taken of temperature rise in the various components as a function of time. Figure 4-5 shows typical temperature behavior at 100A (limited by the power supply used in the test). In the experiment the stainless resistors had a resistance of ~0.04Ohm, twice that of the actual system. A similar test on the same resistor without the Copper thermal connection resulted in burnout of the resistor in less than 30 seconds. The experiment demonstrated two key characteristics of the modified system:

1. The added Copper components allow for current transport through the bypass resistors over long times, eliminating the risk of conductor burnout during serious fault conditions;
2. Significant heat is transferred to the cold mass Al components, which will result in quench initiation in neighboring coils in a much shorter timescale that in the baseline system design.

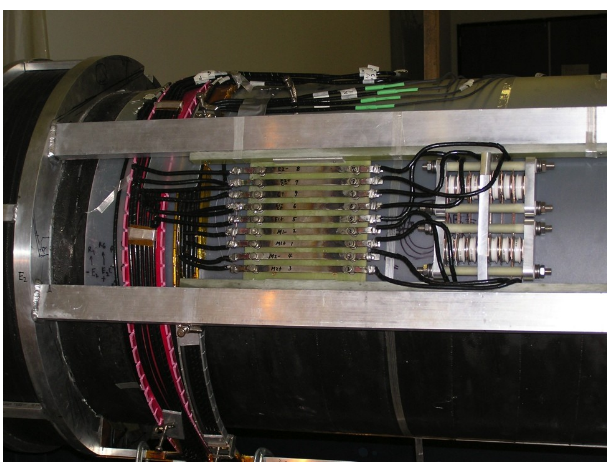

Figure 4- View of the passive protection system as initially designed and installed on the MICE spectrometer solenoid system.

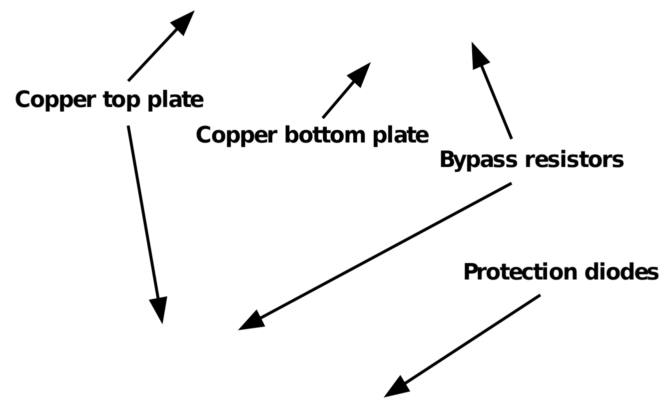

Figure 4- Conceptual design of a thermal link from the protection resistors to the cold mass structure. The copper top plate is in direct contact with the Aluminum side-rails in the coil housing; the bottom plates act to "sandwhich" the resistors, which are insulated from the copper using ceramic cloth.

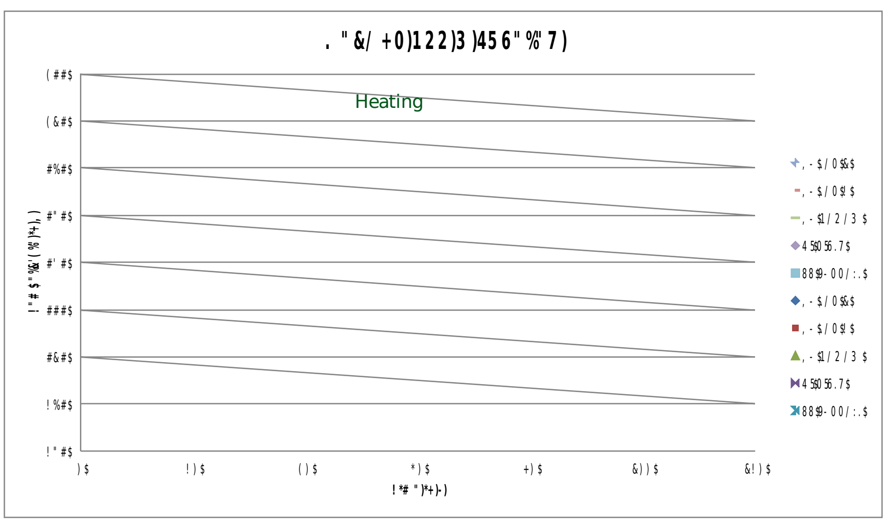

Figure 4-. Temperature-rise vs time for components of the modified protection circuitry. Note that significant temperature rise is evident in the Aluminum side-rails within a minute of the introduction of current.

4.2. HTS lead protection

The existing system does not provide protection of the HTS leads. In the case of an HTS lead quench, the voltage across the lead will rise. We intend to add an external (warm) circuit composed of a switch and a ~0.2 Ohm resistor across each pair of leads; activating the switch and turning off the power supply will result in a driving voltage sufficiently large to trip the cold diodes, resulting in a parallel current path and a dramatic reduction in current through the (quenching) HTS leads. The system will protect the leads except under a fault scenario where the active detection fails.

ADD SKETCH OF MODIFIED CIRCUIT

5. Conclusions

A systematic analysis of quench scenarios has been performed to validate the general magnet design in terms of hot-spot temperatures, internal voltages, and the role and reliability of quenchback propagating quenches through the spectrometer solenoid coils. Under normal operating conditions the systems magnet protection system is found to function correctly, with any one coil quench resulting in a sequence of coil quenches that largely deposit the stored magnetic energy in the coils in the form of heat, with hot-spot temperatures not exceeding ~130K. Furthermore, the internal voltages are acceptable, with adequate turn, layer, and ground insulation in the coilpacks.

The protection system has already been subjected to, and survived, serious fault scenarios, including two different lead burn-out cases. Inspection of the coil protection system suggested the system was marginally adequate to protect the cold mass. A simple modification to the existing system is proposed that will mitigate the large temperature rise in the bypass resistors under fault conditions, and aid in initiating and propagating quenches if a fault should occur.

A modification to the external circuit design is proposed to protect the HTS leads. The design requires detection of increased voltage drop across the leads and the active triggering of an external switch. By appropriate selection of external resistance the circuit will result in a significant reduction in current through the HTS leads and protect them from burn-out.

Appendices:

I. Material properties

All the materials' properties will be stored in table files, which will be loaded into the finite element model. For quench analysis, two kinds of properties are required: (1) thermal properties; (2) electrical properties. Thermal properties include thermal conductivity, specific heat; electrical properties include resistivity and critical data of superconductor.

I.1 Thermal conductivity

Thermal conductivity is a kind of transportation properties. A coil winding is essentially a compound structure made of turns and insulations as shown in Fig I-1. The interlayer insulation is fiberglass and epoxy; we use G-10 to simplify. The turn-to-turn insulation is just epoxy. The RRR value of the copper is 70. Each turn and its insulation is the basic element of a coil winding. The equivalent transportation properties of a compound material can be obtained from such basic cells.

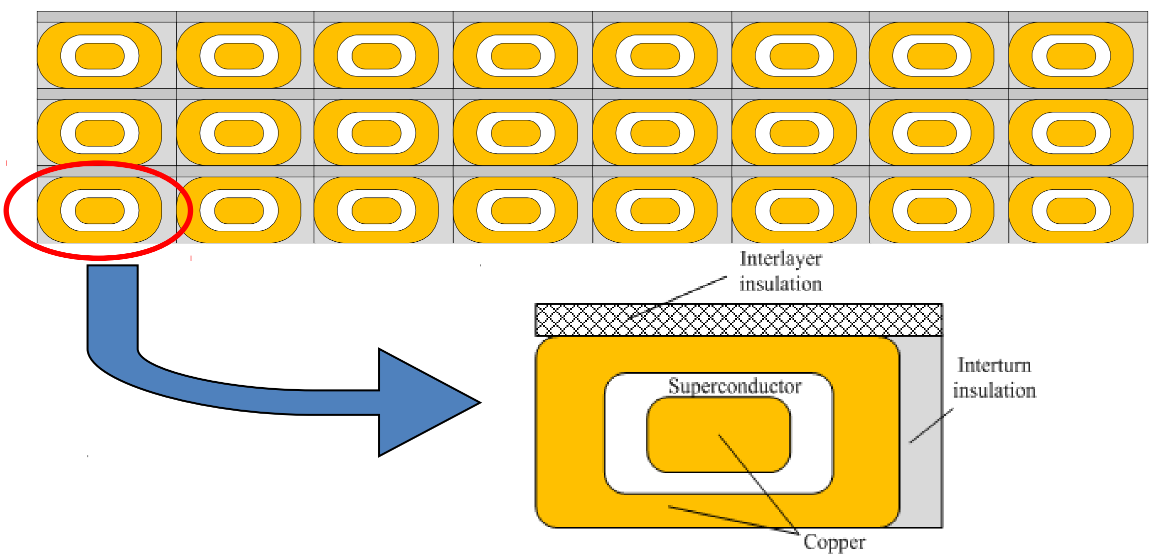

Figure I-1 Schematic diagram of a coil cross section

The approach to calculate the effective thermal conductivity of a coil is thermal resistance network method. The heat flow goes through a basic cell is analogy to current, and temperature is analogy to voltage drop. The thermal resistance is basically expressed by:

$$R = \frac{\delta}{\lambda \cdot A} \quad \text{(I-8)}$$

δ is the thickness; λ is the effective thermal conductivity; A is the heat flow area. For a 2D problem, A can be replaced by length. For detailed calculation, the basic cell will be separated into several parts along the heat flow path; each part is a thermal resistor, all the resistors form a thermal resistance network (Figure I-2). The total resistance of the basic cell is:

$$R_r = \frac{1}{\frac{1}{R1+R2+R3+R4+R5} + \frac{1}{R10+R11+R12} + \frac{1}{R6+R7+R8} + \frac{1}{R9} + \frac{1}{R13} + \frac{1}{R14}} + R15$$

(I-9)

Combined expressions (I-1) and (I-2), one can get the equivalent thermal conductivity in the radial direction.

Figure I-3 Thermal resistance of each cell in radial and axial directions

The same approach is used to obtain the thermal conductivity in the longitudinal direction. In the azimuthal direction the thermal conductivity of a coil structure is dominated by the copper properties. Therefore, the thermal conductivity of coil in hoop direction is equal to the thermal conductivity of copper times its volume fraction.

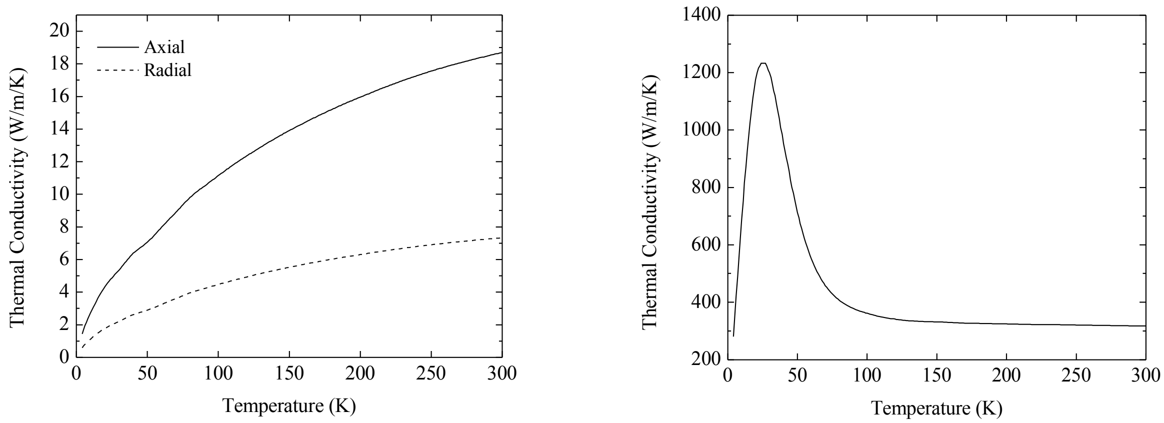

Figure I-3 Effective thermal conductivity of coil in transverse directions and azimuthal direction

The thermal conductivity of mandrel (6061 Al) is obtained from Cryocomp database.

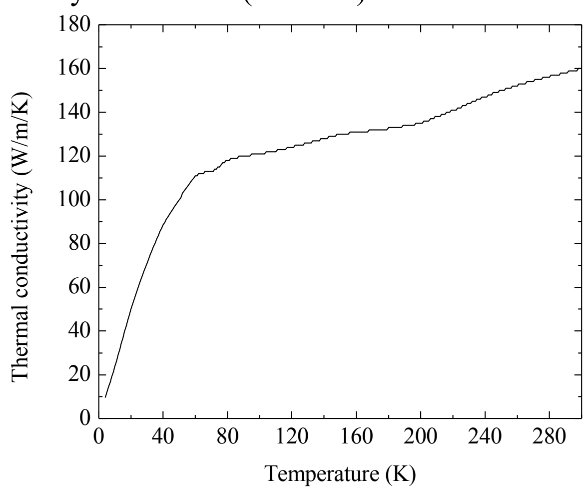

Figure I-4 thermal conductivity of 6061 aluminum

I.2 Heat capacity

Heat capacity of coil winding can be also obtained by compound material method. The expression of specific heat capacity is:

$$Cp_{coil} = \frac{Cp_{NbTi} \cdot \rho_{NbTi} \cdot 0.2 + Cp_{Cu} \cdot \rho_{Cu} \cdot 0.8}{\rho_{coil}} \quad \text{(I-10)}$$

Cp_{NbTi} is the specific heat of NbTi alloy; ρ_{NbTi} is the density of NbTi alloy, 6550 kg/m^3. Cp_{Cu} is the specific heat of copper; ρ_{Cu} is the density of copper, 8960 kg/m^3. ρ_{coil} is the density of coil, 8478 kg/m^3. The heat capacity of mandrel (6061 Al) is also from Cryocomp database.

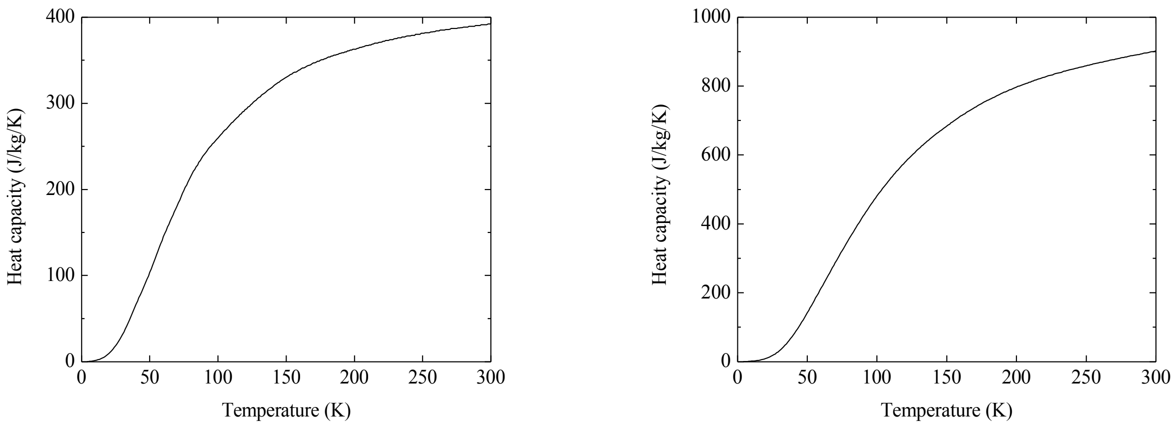

Figure I-5 Heat capacity of coil winding and 6061 aluminum mandrel

I.3 Critical data of superconductor

Critical data set is extremely important for quench simulation. The VF QUENCH code loads critical data for a given conductor to determine the transient state of conductor during quench process.

Fitting formulae for critical surface of superconductor are very commonly used for engineering calculation. The expressions in this note have a very good fitting agreement with test results and are verified by literatures [1].

The main expression is:

$$J_c(T,B) = C_0 \cdot \frac{B^{\alpha-1}}{B_{c0}^{\alpha}(1-\frac{T^n}{T_{c0}^n})^{\alpha}}[1-\frac{B}{B_{c0}(1-\frac{T^n}{T_{c0}^n})}]^{\beta}(1-\frac{T^n}{T_{c0}^n})^{\gamma} \quad \text{(I-11)}$$

The constant coefficients in formula I-4 are determined by the test results of short sample. For MICE project, the bare conductor has a cross area of 1.6mm*0.95mm, and a Cu/NbTi ratio of 3.9:1, the measurement data at 4.2K are:

Table I-2 short sample measurements at 4.2K

B (T)	Ic (A)
4	1050
5	872
6	699
7	522
8	349

From test results, the constants in the expression above are indentified as listed in Table I-2:

Table I-3 Parameters of the fitting formula

α	0.7
β	1

γ	2.2
C_0	28*J_c(4.2K,5T)
J_c(4.2K,5T)	2.588E9 (A/m^2)
B_{c0}	14 T
T_{c0}	10 K

By using the formula I-1 and the proper coefficients, one can get the critical surface in 0~10K and 0~6T.

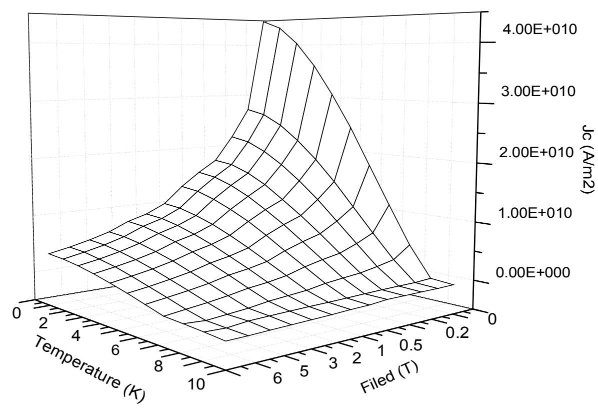

Figure I-6 Jc surface of MICE conductor

I.4 Resistivity of materials

The resistivity of each material is used to calculate Joule heat and eddy current in quench process. The resistivity of copper and 6061 aluminum is from Cryocomp database.

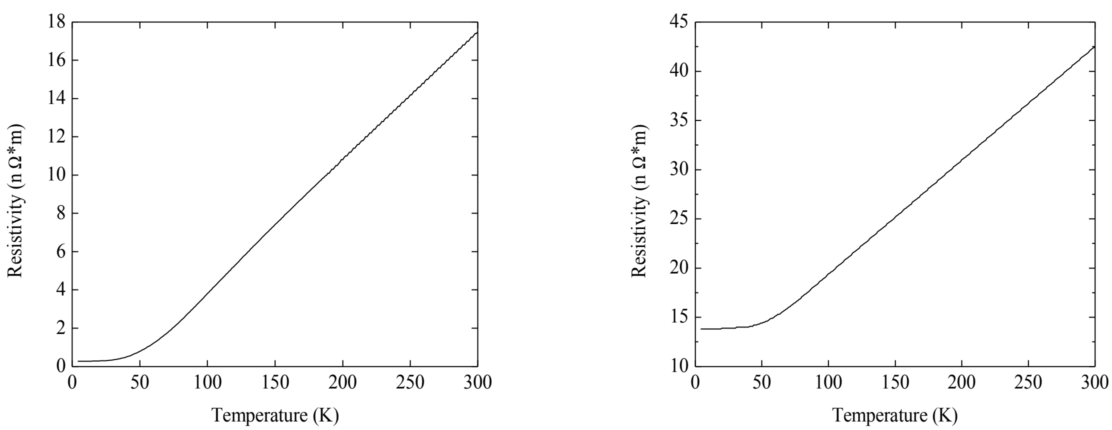

Figure I-7 Resistivity of copper and 6061 aluminum

II. Code validations

II.1. Validate a simple model by Wilson code and hand calculation

In order to validate the reliability of the finite element model, we have carried out a sensitive test by using Wilson code and hand calculation.

A simple finite element model just containing the central coil and its protection circuit was built to check the hot spot temperature and current decay. The central coil in this test model is also separated into two sections in radial direction.

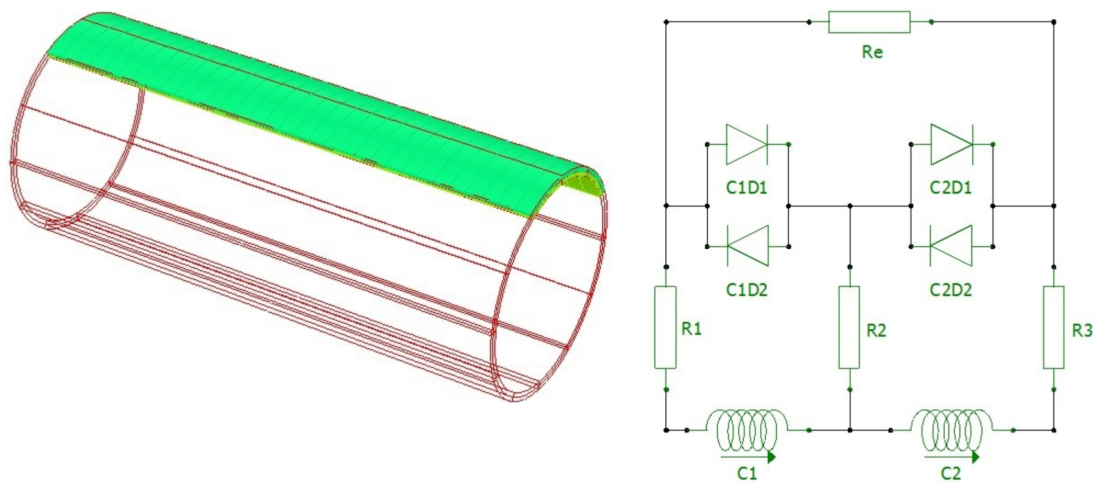

Figure II-4 Simple test model and protection circuit

The bypass resistors and cold diodes are same as used in the formal finite element model. The initial current is 265A, a quench was triggered in the inner surface at one end of the coil. The mutual inductances of the two sections are:

Table II-4 Mutual inductance of the two sections (H)

	C1	C2
C1	10.717	10.8
C2	10.8	11.562

The same scenario is performed by a 2D FORTRAN code based on Wilson quench theory. In this code, each coil section is assumed to be adiabatic; a quench is initiated in the same place as the test model and starts to expand in the transverse directions with average constant velocities v_r (radial propagation) and v_z (axial propagation). The normal zone shape is assumed to be an ellipsoid; at each time step another layer is added to the surface of the normal zone like the skin of an onion. The calculation continues until each coil subdivision current is less than the 1 percent of its initial current.

In this semi-empirical model, the quench propagation velocities in transverse directions need to be pre-defined. The equations to calculate propagation velocities are fitting expressions based on the potted coil experimental quench velocity points [[2],[3]]:

$$v_\theta = (5.7 \times 10^{-14})(1+B)^{0.62} J^{1.65} \qquad \text{(II-12)}$$

v_θ is velocity along conductor, which is determined by the average filed and the operation current density. From v_θ, one can estimate the transverse velocities using the following relations:

$$v_r = \alpha v_\theta \,, v_z = \beta v_\theta \qquad \text{(II-13)}$$

Where, r means radial direction, and z means longitudinal direction. The coefficients of α and β are expressed:

$$\alpha \approx 0.7\left[\frac{\rho_n k_i}{LT_c}\frac{b}{S}\frac{r+1}{r}\right]^{0.5}, \beta \approx 0.7\left[\frac{\rho_n k_i}{LT_c}\frac{a}{S}\frac{r+1}{r}\right]^{0.5} \qquad \text{(II-14)}$$

In equations II-3, L is the Lorentz number (L = 2.45*10^{-8} ΩWK^{-2}.); k_i is the thermal conductivity of the insulations; T_c is the critical temperature (10 K); and ρ_n is the resistivity of copper. S is the total insulation thickness; a is the total length of the conductor (in the z direction); b is the total thickness of the conductor (in the r direction); and r is the copper to superconductor ratio (3.9).

The average filed is about 3.5T, so, the velocities in transverse directions are: v_r =0.106 m/s and v_z =0.165m/s.

Figure II-2 shows the comparison of results. These two kinds of model have a fair agreement in current decay and hot spot temperature. The Wilson code uses some empirical expressions, which may cause some differences in current decay rate and temperature distribution.

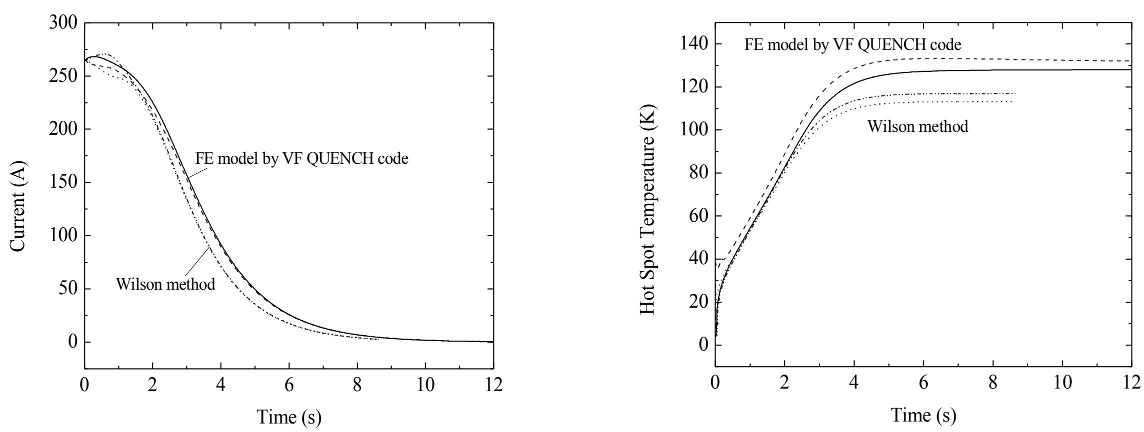

Figure II-5 results of FE model and Wilson model

A sensitive test by using hand calculation was performed to validate the accuracy of the finite element model. This sensitive test is based on energy equilibrium. The stored energy of the coil will be dissipated into the coil itself and resistors to make temperature rising. Therefore, the absorbed energy is:

$$Q_a = \sum_{i=1}^{N} m_i \int_{4.2}^{T_i} Cp(t)dt \qquad \text{(II-15)}$$

In equation II-4, N is the total turns of the central coil. m_i is the mass of each turn and its insulations; T_i is the final temperature of each turn at the end of quench; Cp is the bulk heat capacity of coil winding. The stored energy is expressed by:

$$Q_s = \frac{1}{2} LI^2 \qquad \text{(II-16)}$$

L is the self inductance of the central coil, which is about 43.7H. I is the operation current of 265A. The bypass resistors in the FE model have a resistance of 0.02Ω. The integral Joule heat of these resistors in the quench process is about 6000 J. Q_s is equal to 1.53 MJ, and Q_a is equal to 1.52 MJ, so the Q_a +6000 J ≈ Q_s.

We also considered a worst case that the initial position of quench is adiabatic. Thus this point will get the highest temperature in the coil.

$$d_c \cdot \frac{\beta+1}{\beta} \cdot \int_{4.2}^{T} \frac{Cp(t)}{\rho(t)} dt = \int_{0}^{ts} J_0^2(\tau)d\tau \qquad \text{(II-17)}$$

Where, d_c is the density of coil winding; β is copper superconductor ratio. ρ is resistivity of copper. J_0 is transient current density in copper. ts is duration of quench. The maximum temperature from equation II-6 is 137K, which is a bit higher than peak value of FE model. So, the Wilson code and hand calculation proved that the FE model is reasonable.

II.2. Validate the influence of mesh and time step

Bad mesh may cause problems in convergence. In the formal finite element model, different levels of mesh refinement were applied. For coil and mandrel, we used finer mesh; for air region near the cold mass, we used the same level of mesh as did in coil; for further air region, we used lower level of mesh. Doing so is to reduce computation and save time.

A triplet coils model was built to verify the influence of mesh refinement. The triplet model consists of E1, C and E2 coils and 6061 aluminum mandrel as shown in figure II-3.

Figure II-6 Triplet model for validation of mesh refinement

Two cases with different element sizes were performed. One case has a total 27300 tetrahedral elements in coil and mandrel, the element length of the coils is set to be 0.006m in transverse directions; the element length of the aluminum is set to be 0.03m; the element length of the air region adjacent the coils assembly is set to be 0.2m.

The other case has finer mesh, which is same as used in formal finite element model. The amount of element is about 679756, the element length of the coils is 0.003 m; the element length of the coils is 0.02 m. and also refined the mesh in the air region.

The difference of these two cases is shown:

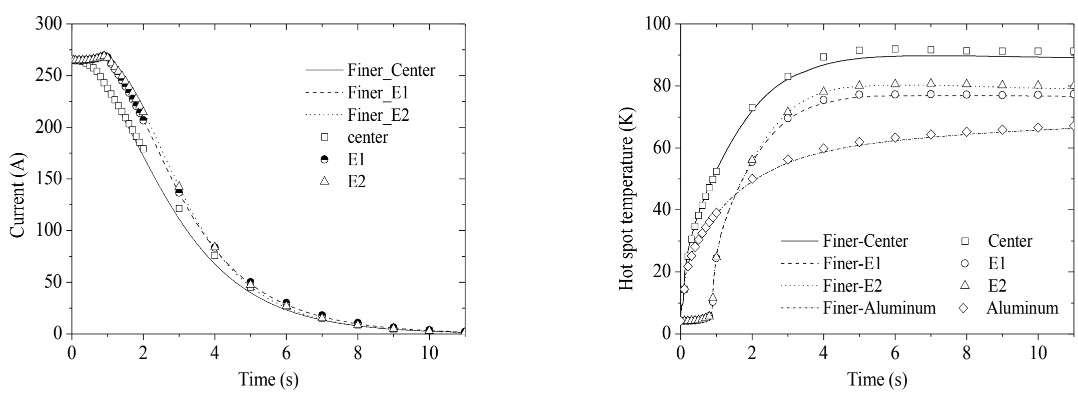

Figure II-7 results with different mesh levels

The results of two cases have a well agreement, however the temperature in the center coil with finer mesh is little higher. The deviations of current and hot spot temperature of the two cases are about 7.04% and 3.01% at 5K, respectively. Finally, the results show mesh in the latter case (also is same in the formal FE model) is sufficiently refined.

Time step also affects results convergence. By using different time steps in formal FE model, one can find the differences if time step is not sufficiently small. Three levels of time steps were tested. They are 0.05s, 0.01s, and 0.005s.

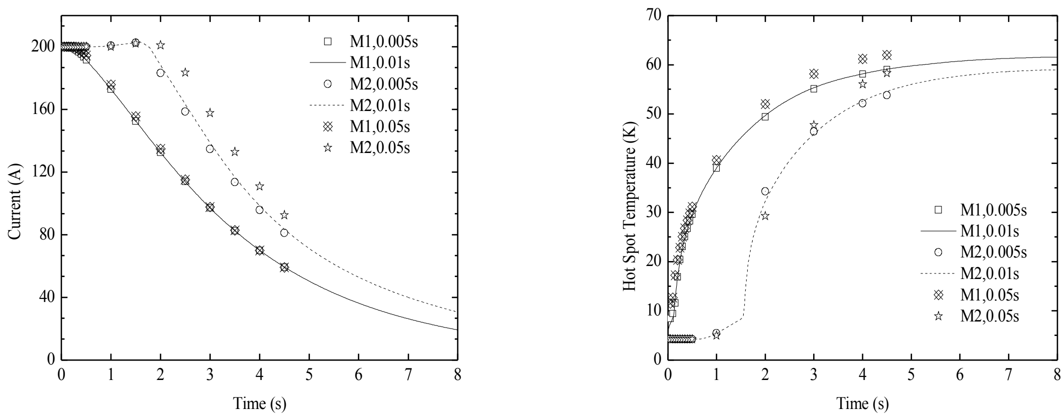

Figure II-8 results with different time steps

Figure II-5 shows the differences between results with these time steps. In this test, M1 coil was triggered quench initially. Using time steps of 0.01 and 0.005s will get close results, while the current with 0.05s time step is a bit larger; Similarly, results of 0.01s and 0.005s have near temperature. Therefore, it is concluded that 0.01s (used in formal FE model) is sufficiently time resolved.

II.3. Validate the difference of point heater and circle heater

The heater type in the model will affect the initial quench propagation. The formal FE model used a circle heater. Circle heater makes simulation just need to a quarter of model. A point heater required at least half model.

A circle heater will cause a 2D quench propagation, and a point heater will cause a 3D quench propagation at the beginning of quench. But when quench-back effect induces quench in the next coil, one can not see any differences in quench propagation. Figure II-6 shows the hot spot temperature in M1 and M2 coils. Using point heater seems to cause a relatively higher temperature in M1 coil, and a longer time delay to trigger M2 coil quench. It may be interpreted that point heater easily to cause heat accumulation and 3D heat transfer may take longer time to conduct heat to mandrel.

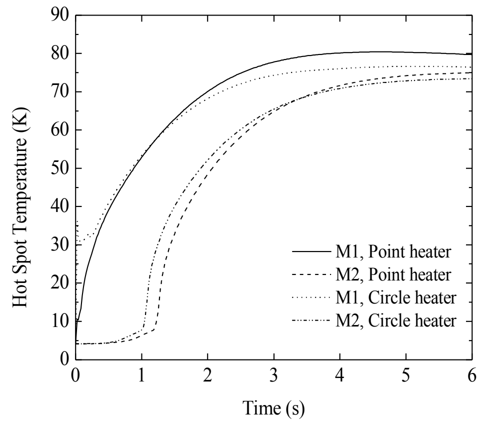

Figure II-9 Hot spot temperature in M1 and M2 coils with point heater and circle heater

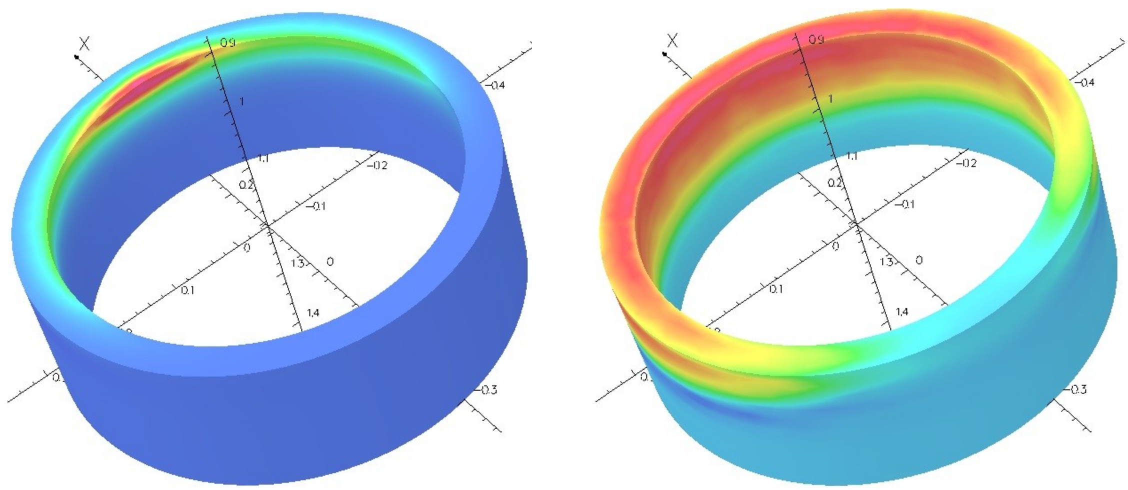

0.1s 0.3s

M1 coil, point heater

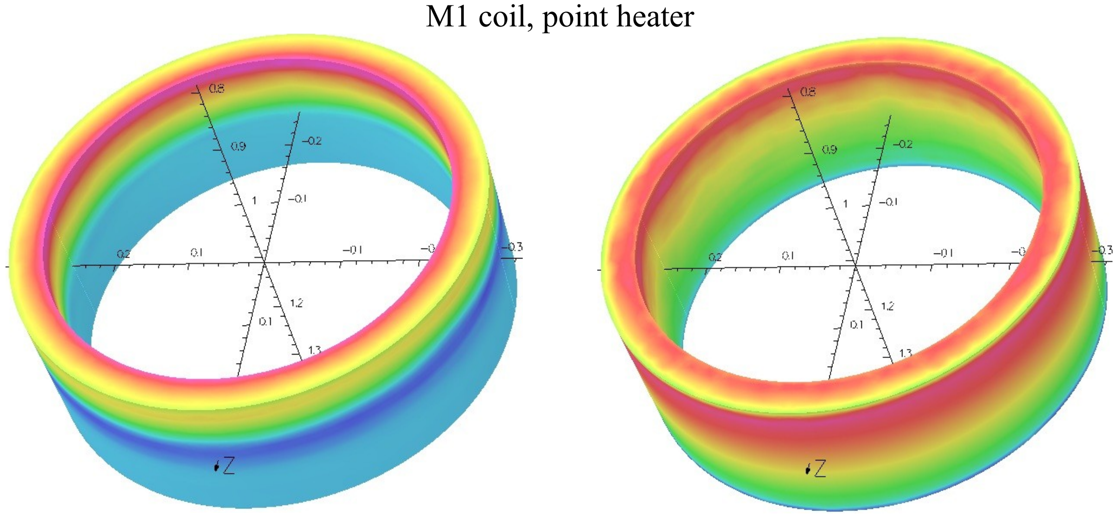

0.1s 0.3s

M1 coil, circle heater

Figure II-10 Temperature contour in M1 coil with point heater and circle heater

II.4. Validate the influence of insulations

The insulations between coil and mandrel will retard heat transfer from normal zone to mandrel; thereby the quench-back will be slowed down correspondingly. While, the normal zone propagation in each quenched coil will not be affected by insulations, so, the consequence of insulations is that the time delay of quench from one coil to the other become longer, and the hot spot temperature in coils is near the results without insulations.

Insulations in model will increase mesh scale. To reduce computation, the formal FE model ignored insulations. To verify the neglecting of insulation will not affect the final results, a model with insulations was created, and applied the same boundary conditions.

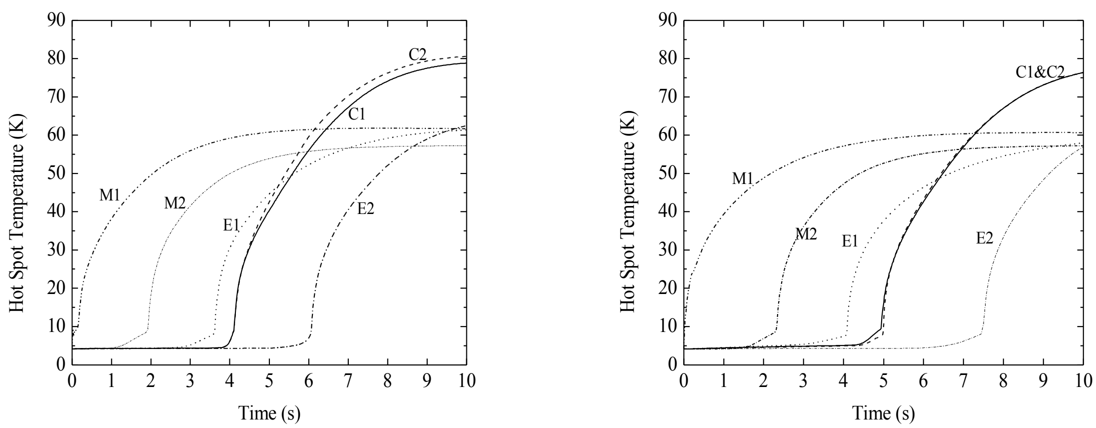

Without insulation With insulation

Figure II-11 Hot spot temperature of formal FE model and insulation model

From figure II-8, one can see the time interval of quench took place in each coil is different. The quench-back slowed down for average 1.3s by insulations. But the hot spot temperature of the two models is very near.

II.5. Validate the influence of different bypass resistors and forward voltage of diode

Bypass resistors will absorb energy from coil during quench. We used the formal FE model to investigate two cases with 0.02Ω and 0.2Ω bypass resistor. The following table shows the hot spot temperature in each coil with different bypass resistors.

Table II-5 Hot spot temperature with different bypass resistors (K)

	C1	C2	E1	E2	M1	M2
0.02Ω	116.35	116.3	79.30	82.29	80.41	75.00

0.2Ω	114.10	114.00	78.15	81.30	79.22	74.15

So, increasing resistance of bypass resistor has made little improvement on reducing hot spot temperature. In fact, more than 90% energy will be dissipated into the coils themselves.

Also, the forward voltage of cold diodes may affect the hot spot temperature in coils. We have checked the results with 4V and 6V forward voltage of diodes, Table II-3 shows the hot spot temperature in each coil of the two cases.

Table II-6 Hot spot temperature with different forward voltage of diodes (K)

	C1	C2	E1	E2	M1	M2
4V	116.35	116.3	79.30	82.29	80.41	75.00
6V	116.10	116.36	78.9	82.97	81.30	76.11

A larger forward voltage will cause a little current delay in diodes, which means a bit more current will go through in the coil with larger forward voltage.

II.6. Validate the influence of linear and nonlinear properties

In Vector Fields Opera 3D software, there are four options for user to define the code behavior when using nonlinear material properties. These four options are: (a) fixed time step + forced linear properties; (b) fixed time step + nonlinear properties; (c) adaptive time step + forced linear properties; (d) adaptive time step + nonlinear properties. “Forced linear properties” means the code would update the non-linear material properties from the current solution at the start of each time step and keep the properties fixed for the time step[[4]], whereas “nonlinear properties” means the code will update the non-linear material properties during the time step.

It is apparently that the option (d) has the most accurate because the adaptive time integration makes sure not only the accurately solving of differential equations in time but also that the rate at which the material properties are changing are not causing errors larger than the adaption tolerance. But this option usually costs more time on solving nonlinear equations.

In fact, option (a) is often the fastest one, but if the fixed time step is too long, the result will not converge or is not reasonable owing to mutation of properties in successive time steps. We have done the comparisons of the results with different options. This test model just contains the subdivided central coil which are meshed by hexahedral elements. The material properties are tabulated functions with temperature. The fixed time step is 0.01s.

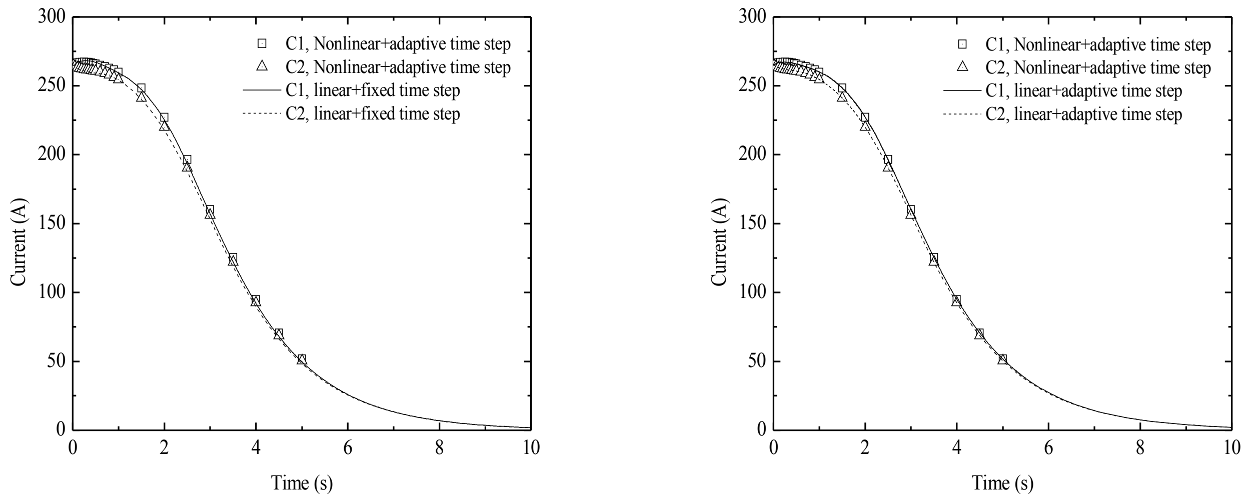

Figure II-12 current decay with option (a) and (d) (left); current decay with option (c) and (d) (right)

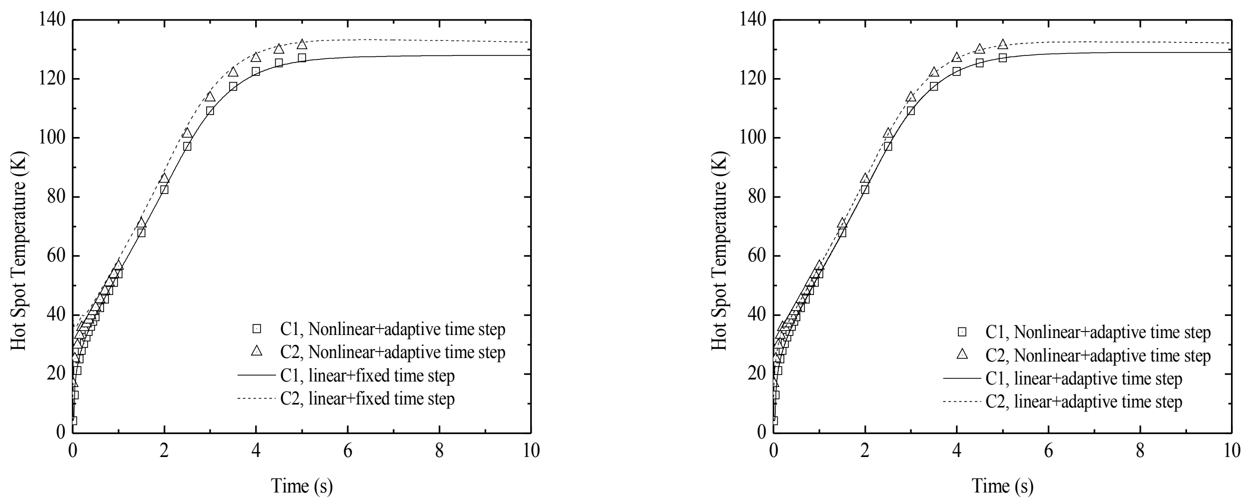

Figure II-13 hot spot temperature with option (a) and (d) (left) ; hot spot temperature with option (c) and (d) (right)

From the comparison, the cases with different options agree fairly well with one another. That means the option (a) also converged with the time step of 0.01s. Thereby, if the time step is sufficient short, the results will be also reasonable, and the benefit of choosing option (a) is that the code will run much faster. So, if one chooses a shorter enough fixed time step, the result should also have good accuracy and more time efficiency.

[1][] L. Bottura. “A Practical Pit for the Critical Surface of NbTi”, *IEEE Trans. Appl. Sup.* , vol.10(1), pp. 1054~1058, 2000.
[2][] M.A. Green, H. White. “Quench Protection and Magnet Power Supply Requirements for the MICE Focusing and Coupling Magnets”, LBNL internal report, LBNL-57580, pp. 4~5, 2005.
[3][] P.H. Elerhard, *et al*. “The Measurement and Theoretical Calculation of Quench Velocities in LARGE Fully Epoxy Impregnated Superconducting Coils”, *IEEE Trans. Mag.*, vol. 17(5), pp. 1803~1806, 1981.
[4][] Jean Marc. Private mail with the Vector Fields technical support, 2011.